Journal of Atomic and Molecular Sciences

ISSN 2075-1303

Global Science Press

Excited state process of a novel NIR-BODI molecule in toluene and acetonitrile solvents: A theoretical study

Received Oct. 26, 2017,
Accepted Dec. 08, 2017,

DOI: 10.4208/jams.102617.120817a

http://www.global-sci.org/jams/

Jia Li[a,b], Meixia Zhang[b], Can Du[b], Peng Song[b,*] and Xiaodong Li[a,*]

Abstract. In this work, using DFT and TDDFT methods, we investigated the excited-state intramolecular proton transfer (ESIPT) mechanism of a novel NIR-BODI system [*Org Biomol Chem* **15**:4072, 2017.] in both toluene and acetonitrile (CH_3CN) solvents theoretically. Comparing the prime structural variations of NIR-BODI involved in the intramolecular hydrogen bond, we can conclude that O-H···N should be strengthened in the S_1 state, which may facilitate the ESIPT process. Concomitantly, infrared vibrational spectra analysis further verify the stability of hydrogen bond. In good agreement with previous experimental results, NIR-BODI reveals two kinds of excited-state structures (NIR-BODI-enol* and NIR-BODI-keto*). Analysis about charge redistribution reveals the tendency of ESIPT process. Our scanned potential energy curves according to variational O-H coordinate demonstrates that the proton transfer process should be more likely to occur in the S_1 state due to the inappreciable potential energy barriers. In addition, due to the minute differences of potential energy curves contrasting toluene (the NIR-BODI-keto could be not located) and CH_3CN (the NIR-BODI-keto can be located) solvents in S_0 state, we deem that solvent effect could play roles NIR-BODI system. Given the S_1-state potential energy barriers, we confirm that the ESIPT process is easier in CH_3CN solvent.

1. Introduction

It is well known that hydrogen bonding plays important roles in many biological and chemical fields [1-4]. Based on the excitation of hydrogen-bonded systems, reorganizations of hydrogen acceptor and donor parts are inevitable due to the primary differences in charge distribution of different electronic states, which could lead to various photochemical and photophysical processes in the excited states [5-9]. Proton transfer (PT) reaction, as one of the most fundamental reactions interrelated with hydrogen bonding, exists in most biological systems such as RNA, DNA, protein environment, and so forth [10, 11]. PT processes have been investigated and explained broadly in the S_0 state, while we focus on the excited state proton transfer (ESPT) reaction, since broad scale applications about ESPT compounds have already become the hot topic via development of novel materials for chemical sensing [12-14], bio-sensing [15, 16], celling imaging [17], white light LED [18-20], and so on.

In general, the excited state intra- or inter- molecular proton transfer (ESIPT) starting from the ground state enol form and returning back to the same state after a so-called "four-level reaction cycle" is reversible [21-25]. Within the frame of ESIPT process, the S_0-state enol could be excited to the excited-state enol*. This form convers into the excited photoproduct (i.e. so-called photo-tautomer keto*), then by the translocation of proton and hence the alteration of the electronic structure. Keto* cold be recognized by the emission spectrum strongly shifted to longer wavelengths. Then the relaxation of keto* results in the S_0-state keto that undergo the reversed proton transfer with the recovery of enol structure to finish the reaction cycle. Experimentally, the fluorescence band of the initial enol* could exhibit a normal Stokes Shift (i.e. the difference between absorption and emission peaks of the enol structure). While the keto* could emit another fluorescence with longer wavelength. Basically, this kind of large Stokes Shift observed in experiment might be as large as 6000 ~ 12000 cm^{-1}.

It is known that the near-infrared (NIR) light could provide the advantages of minimum photodamage to biological samples, decreased interference from the background autofluorescence and deep tissue penetration [26]. The fluorescent dyes owning NIR emission are attributive for the construction of fluorescent imaging

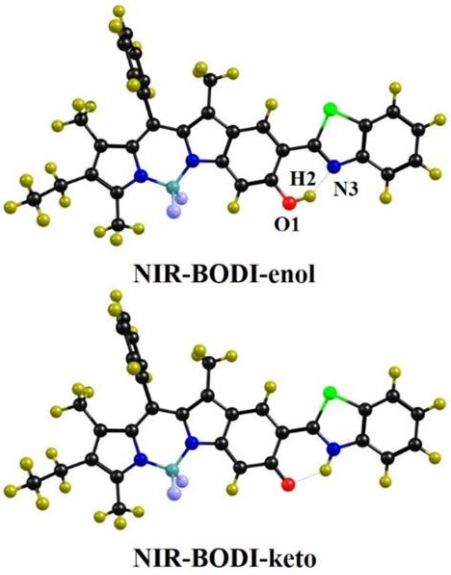

Figure 1: Views of the optimized structures of NIR-BODI-enol and the proton-transfer structure NIR-BODI-keto based on TDDFT/B3LYP/TZVP theoretical level.

[a] *Key Laboratory for Anisotropy and Texture of Materials (Ministry of Education), School of Materials, Northeastern University, Shenyang, Liaoning 110819, E-mail address: xdli@mail.neu.edu.cn*
[b] *Department of Physics, Liaoning University, Shenyang, Liaoning 110036, E-mail address: songpeng@lnu.edu.cn*

sensors. Recently, Fei *et al*. designed and reported a novel NIR fluorescent dye NIR-BODI (see **Figure 1**) system [27]. The significant chemical feature of NIR-BODI is the pre-existing intramolecular hydrogen bond, which could promote the ESIPT process and introduces the NIR fluorescence. Particularly, the free hydroxyl moiety of NIR-BODI could be readily modified to develop novel fluorescent sensors *in vitro* and *in vivo* applications [27]. However, the theoretical investigations about this novel NIR-BODI system is absent, peculiarly, the specific excited state dynamical process is missing in previous experimental work [27]. Furthermore, it is well known that experiments could only provide the indirect information about the photophysical and photochemical properties. The theoretical study about the novel fluorescent NIR-BODI sensor could further deepen the understanding its applications. Therefore, in-depth investigations about the ESIPT reaction of NIR-BODI is necessary. Given the most common theoretical level, the density functional theory (DFT) and time-dependent density functional theory (TDDFT) methods have been widely used to clarify fundamental aspects about different electronic states. In this present work, we mainly focus on studying the ESIPT mechanism based on DFT and TDDFT methods. Bond lengths and bond angles about the intramolecular hydrogen bond as well as homologous infrared (IR) vibrational spectra have been analyzed in detail. Based on the photoexcitation, the frontier molecular orbitals (MOs) and corresponding Mulliken's as well as NBO charge distribution analysis explore the charge redistribution, which reveals the tendency of ESPT reaction. At last, the constructed S_0 and S_1 states potential energy curves indicate the direct information about NIR-BODI sensor.

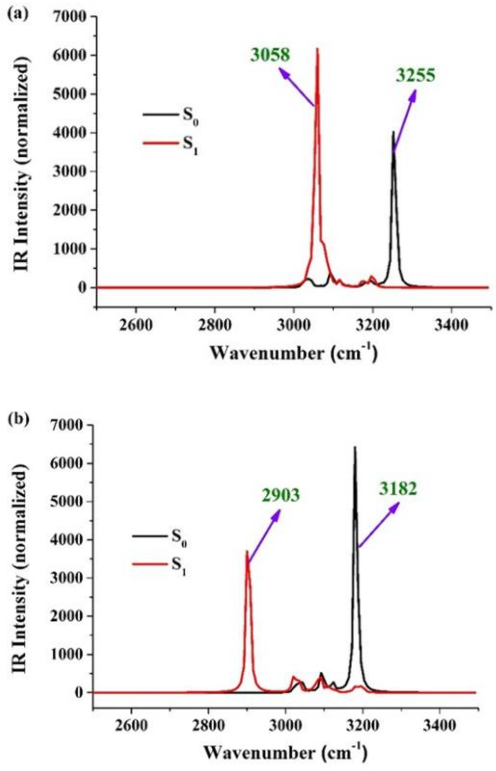

Figure2: The theoretical IR spectra of NIR-BODI-enol structure in both toluene (a) and CH_3CN (b) solvents at the spectral region of corresponding O1-H2 bond in both S_0 and S_1 states.

Our paper is organized such as that the next section describes the details of the Computational Details. Then the Results and Discussion part shows and discusses our theoretical results, and is organized by subsections that consider geometries, electronic spectra, frontier molecular orbitals and the analyses of mechanism. A final section summarizes and provide the conclusions of this present study.

2. Computational Details

In the present work, all the electronic structure calculations have been carried out depending on the Gaussian 09 program suite [28]. The geometric optimizations of the NIR-BODI were performed in the ground state using density functional theory (DFT) method and the electronic excited state was performed depending on time dependent DFT (TDDFT) method, respectively. Becke' three-parameter hybrid exchange functional with Lee-Yang-Parr gradient-corrected correlation (B3LYP functional) was used in both the DFT and TDDFT methods [29-31]. The triple-ζ valence quality with one set of polarization functions (TZVP) was chosen as basis sets throughout, which is an appropriate basis set for this system. There were no constraints to all the atoms, bonds, angles or dihedral angles during the geometric optimization. To evaluate the solvent effect, according to previous experiment [27], toluene and acetonitrile (CH_3CN) were used as solvent in the calculations depending on the model that the Polarizable Continuum Model (PCM) using the integral equation formalism formalism variant (IEFPCM) [32-34]. All the local minima were confirmed by the absence of an imaginary mode in vibrational analysis calculations. The S_0 and S_1 potential energy curves have been scanned by constrained optimizations in their corresponding electronic state, and keeping the O-H distances fixed at a serious of values.

3. Results and discussion

The structures of ground state and the first excited state of NIR-BODI chromophore have been obtained based on B3LYP functional with TZVP basis set level of theory, with a subsequent vibrational frequency analysis to ensure the validity of the stationary points. Both toluene and CH_3CN solvents were used in the IEFPCM model insuring consistency with previous experiment. After optimizations, we found two kinds of configurations of NIR-BODI sensor (i.e., NIR-BODI-enol (the normal NIR-BODI structure) form and NIR-BODI-keto (the proton-transfer NIR-BODI structure) form) in both S_0 and S_1 states (see **Figure 1**). Within the framework of AIM theory (manly based on the analysis of electron density at the specific point (ρ

Table 1: The calculated bond lengths (Å) and angles (º) for NIR-BODI-enol and NIR-BODI-keto forms in S_0 and S_1 states based on the DFT/TDDFT methods with IEFPCM (toluene and CH_3CN), respectively.

	Toluene				CH_3CN			
	NIR-BODI-enol		NIR-BODI-keto		NIR-BODI-enol		NIR-BODI-keto	
	S_0	S_1	S_0	S_1	S_0	S_1	S_0	S_1
O1-H2	0.990	0.992	-	1.829	0.993	1.009	1.602	1.842
H2-N3	1.732	1.726	-	1.026	1.708	1.650	1.061	1.025
δ(O1-H2-N3)	146.29˚	146.89˚	-	131.4˚	148.18˚	148.62˚	140.71˚	130.85˚

(r))), identification of a critical point (CP) and the existence of a bond path in equilibrium geometry are necessary and sufficient conditions for assigning an interaction between two primary atoms [35, 36]. And the AIM analysis of the title compounds ensure the presence of an appreciable interaction between the atoms concerned. The relevant AIM topological parameters involved in the optimized geometries demonstrate that the ρ(r) at the bond critical point (BCP) for NIR-BODI-enol system are close to 0.04 a.u. (the maximum threshold value proposed by Popelier to ensure the presence of hydrogen bond [35, 36]. What is more, the corresponding $\nabla^2\rho_c$ values are also in the range (0.02 ~ 0.15 a.u.) [35, 36]. Therefore, we can confirm that all these intermolecular hydrogen bonds should be formed for NIR-BODI-enol complex.

The primary structure parameters of NIR-BODI system, such as bond lengths and bond angles, have been listed in **Table 1**. For NIR-BODI-enol form, it can be found that the O1-H2 bond is lengthened from S_0-state 0.99 Å to S_1-state 0.992 Å in toluene solvent, and that the hydrogen bond H2···N3 is shortened from 1.732 Å to 1.726 Å. Similarly, in CH_3CN solvent, bond lengths own larger changes (i.e., upon the excitation, O1-H2 bond is elongated from S_0-state 0.993 Å to S_1-state 1.009 Å, while hydrogen bond H2···N3 is shortened from 1.708 Å to 1.650 Å.). Furthermore, the bond angle δ(O1-H2···N3) is also increased in both toluene and CH_3CN solvent in S_1 state. That is to say, based on the photo-excitation, the intramolecular hydrogen bond O1-H2···N3 of NIR-BODI-enol form should be strengthened in the S_1 state [37-41], which provides the possibility of the ESIPT reaction [42-50]. And comparing these two kinds of solvents, it should be noticed that O1-H2···N3 could be affected larger in CH_3CN one. In addition, it is interesting to find that the proton-transfer NIR-BODI-keto form could not be located in toluene, whereas this structure could be found in CH_3CN solvent.

In addition, the electronic excited-state hydrogen bonding interactions could be detected based on the spectral shift with corresponding special vibrational modes [37-41]. Therefore, we theoretically studied the infrared (IR) vibrational spectra of NIR-BODI-enol in both toluene and CH_3CN solvents as shown in **Figure 2**. One thing should be noted that the ground-state vibrational mode of O1-H2 moiety in toluene solvent is located at 3255 cm^{-1}, while it changes to be 3058 cm^{-1} in the S_1 state. The stretching band owns a red shift of 197 cm^{-1} in the S_1 state relative to S_0 state, which indicates that the intramolecular hydrogen bond O1-H2···N3 of NIR-BODI-enol should be strengthened in the excited state. In a similar way, in CH_3CN solvent, a larger red shift (279 cm^{-1}) could be resulted in based on the photo-excitation from S_0-state 3182 cm^{-1} to S_1-state 2903 cm^{-1}. That is to say, polar CH_3CN solvent do largely affect the excited state hydrogen bonding dynamics of NIR-BODI system. And the strengthening intramolecular hydrogen bond could facilitate the ESIPT reaction in the S_1 state.

Based on the TDDFT/B3LYP/TZVP calculated level, the corresponding peaks of absorption and fluorescence spectra of NIR-BODI structures have been listed in **Table 2** in both toluene and CH_3CN solvents. It is worth mentioning that an intense $S_0 \rightarrow S_1$ transition for NIR-BODI-enol is predicted at around 541.85 nm in toluene and at 515.53 nm in CH_3CN, which are good reproductions of experimental results (570 nm and 546 nm) [27], respectively. In addition, the normal emissions of NIR-BODI-enol form are 619 and 615 nm in toluene and CH3CN solvents, which are also close to experimental 586-600 nm [27]. Given the emissions of NIR-BODI-keto form, the fluorescence is 822 nm in toluene and 790 nm in CH_3CN, which are consistent with experimental 808 and 765 nm, respectively [27]. Even though some differences (less than 30 nm) between previous experiment and our calculated electronic spectra,

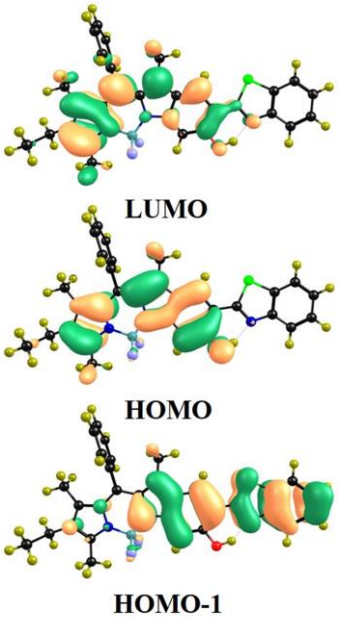

Figure3: View of frontier molecular orbitals (HOMO-1, HOMO and LUMO) for NIR-BODI-enol form.

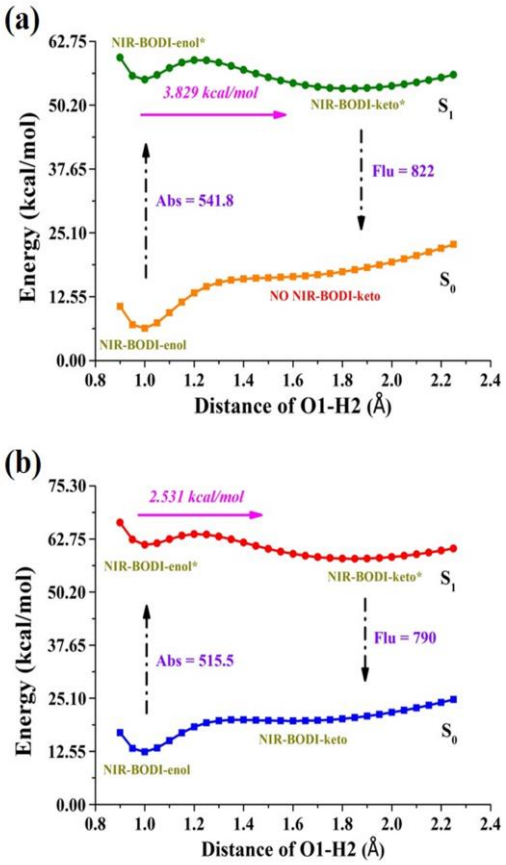

Figure 4: The constructed potential energy curves for NIR-BODI system in toluene (a) and CH_3CN (b) solvents in S_0 and S_1 states.

the NIR emission results in a large Stokes shift around 200 nm, which is in complete agreement with experiment. Herein, we want to mention that these little differences of spectra resulting from theoretical method, which is nothing strange.

In addition, it is well-known that charge distribution over the studied molecule can be changed upon the process of photo-excitation, which effectively has an effect on excited-stated dynamics [51-60]. Especially, the frontier molecular orbitals (MOs) can provide information about properties of excited-stated structures on qualitative discussions of charge distribution. Therefore, in this part, we mainly focus on the excitation process in both toluene and CH_3CH solvents. The calculated electronic transition energies and relative oscillator strengths as well as the compositions have been shown in **Table 3**. Clearly, the S_0-S_1 state transition mainly corresponds to the highest occupied molecular orbital (HOMO) to the lowest unoccupied molecular orbital (LUMO). It can be assigned as a dominant ππ* type transition from with the percentage around 90% (shown in **Figure 3**) in both toluene and CH_3CH solvents. It should be noticed that the electron density of N3 atom increases, while that of O1 atom decreases upon the transition from HOMO to LUMO. And quantitative electron density changes of primary atoms were also calculated in our present work. Due to the similar changing trend of charge redistribution in toluene and CH_3CN solvents, herein, we just provide the results in toluene solvent. Based on analysis of Mulliken's charge distribution, we found that the contribution of N3 atoms increases from 1.056% to 5.194%, while that of both O1 atom drops from 7.864 % to 4.189 %. That is to say, increased electron density of N3 atoms could enhance intramolecular hydrogen bond O1-H2···N3, which should promote the ESIPT process.

To further understand the PT mechanism deeply, both the ground state and the first excited state potential energy curves have been scanned, which is based on constrained optimizations in their corresponding electronic states with keeping the O1-H2 distance fixed at a serious of values. Although the TDDFT/B3LYP calculated level may not be expected to be accurate sufficiently to surmount the correct ordering of the closely spaced excited states, researches have indicated that this method may be reliable previously as far as the shape of hydrogen-transfer potential energy curves is concerned [61, 62]. The potential energy curves with only the variable parameter of O2-H8 bond length from 0.90 to 2.25 Å in steps of 0.05 Å including NIR-BODI-enol and NIR-BODI-keto geometries in both toluene and CH_3CN solvents (shown in **Figure 4**), which should provide qualitative energetic pathways for the ESIPT process of NIR-BODI chromophore. One thing should be noticed that the potential energy curve of S_0-state NIR-BODI is increased ceaselessly in toluene, which confirms that there is not NIR-BODI-keto form located in the S_0 state. Otherwise, in CH_3CN solvent, the NIR-BODI-keto could be located in the S_0 state. Obviously, the solvent plays important roles in NIR-BODI system. Even though NIR-BODI-keto can be found, the potential energy barrier in the S_0 state hinders PT reaction. Given the S_1 state, it is worthwhile noticing that the first excited state potential energy curves exhibit lower potential energy barriers between the reagent enol* (from the vertical transition at the geometry of the minimum in the ground state) and the product keto*. That is to say, transferring the proton H2 from O1 to N3 for NIR-BODI-enol overcomes a very low barrier in the S_1 state, thus indicating that the ESIPT is more likely to be proceeded than GSIPT. In addition, it can be found clearly in **Figure 4** that the enlarged potential energy curves constructed keeping O1-H2 bond length in step of 0.05 Å reveal the barrier (3.829 kcal/mol) in toluene solvent is higher than that of 2.531 kcal/mol in CH_3CN solvent. It might be explained by the different changes of hydrogen bonding bond lengths in these two solvents as mentioned above, since the intramolecular hydrogen bond O1-H2···N3 seems to be more active based on photo-excitation. The implication is that solvent effects can more or less regulate and control excited state behaviors of NIR-BODI system. For further revealing the changing tendency bringing from solvents, we also add three other solvents (cyclohexane, chloroform and DMSO). It is well known that the polarity of cyclohexane is lower than toluene, that of chloroform is between toluene and CH_3CN, and that of DMSO is higher than CH_3CN solvent. Our theoretical potential energy barriers for cyclohexane, chloroform and DMSO are 4.173, 3.186 and 2.514 kcal/mol. That is to say, we further reveal that the ESIPT reaction of NIR-BODI can be controlled by solvent polarity, namely, polar aprotic organic solvents can facilitate the ESIPT process for NIR-BODI. Therefore, we conclude the ESIPT process and mechanism as follow: Upon the excitation, the NIR-BODI-enol structure in the S_0 state can be excited to the NIR-BODI-enol* form in the S_1 state, then, ESIPT process occurs with crossing a lower potential barrier forming the NIR-BODI-keto* form in the S_1 state. Subsequently, the NIR-BODI-keto* decays back to the ground state through radiating fluorescence, which induces the distinct bathochromic shift in their fluorescence emission spectra as compared with that of NIR-BODI-enol* structure. The NIR-BODI-keto can also undergo the reverse GSIPT process back to NIR-BODI-enol. In addition, due to the differences of potential energy curves in both S_0 and S_1 states, we believe that solvent effect could play roles in controlling excited state behaviors of NIR-BODI system.

Table 2: The calculated absorption and fluorescence peaks for both NIR-BODI-enol and NIR-BODI-keto structures in both toluene and CH_3CN solvents based on TDDFT/B3LYP/TZVP level.

	NIR-BODI-enol		NIR-BODI-keto
	Abs.	Flu.	Flu.
Toluene	541.85	619	822
CH_3CN	515.53	615	790

4. Conclusions

In summary, based on the DFT/TDDFT method, the ESIPT

Table 3: The theoretical electronic excitation energies (nm), corresponding oscillator strengths and corresponding compositions for NIR-BODI-enol chemosensor in both toluene and CH_3CH solvents.

	Transition	λ (nm)	f	Composition	CI (%)
Toluene	S_0-S_1	541.85	0.6306	H → L	88.93%
				H-1 → L	10.03%
	S_0-S_2	506	0.6141	H-1 → L	87.22%
CH_3CN	S_0-S_1	515.53	0.6648	H → L	88.51%
				H-1 → L	10.26%
	S_0-S_2	491	0.5099	H-1 → L	86.62%

mechanism of the NIR-BODI system has been investigated in both toluene and CH_3CN solvents. We testified the intramolecular hydrogen bond O1-H2···N3 should be formed in the S_0 state. The phenomenon of hydrogen bond strengthening in the S_1 state based on primary bond lengths, bond angles and IR vibrational spectra indicated the tendency of excited state proton transfer. In addition, the DFT/TDDFT method we adopted reappeared the absorption and fluorescence spectra reported in the experiment, which demonstrated that the TDDFT theory is reasonable and effective for this chromophore. The corresponding frontier molecular orbitals have been analyzed manifesting the ESIPT process could happen due to the intramolecular charge transfer. The constructed potential energy curves of the S_0 state and S_1 state demonstrated that the proton transfer are more likely to happen in the S_1 state due to the relative lower barrier. That is to say, the ESIPT was facilitated based on the photoexcitation legitimately. In the end, comparing the potential barriers in toluene and CH_3CN solvents, we conclude that solvent effect could regulate and control excited state behaviors of NIR-BODI system.

Acknowledgements

This work was financially supported by the Innovative Talent Support Program of Liaoning Province (Grant No. LR2017062), the Liaoning Provincial Department of Education Project (Grant No. LFW201710), the Natural Science Foundation of Liaoning Province (Grant No. 201601095 and 201602345), and the program of the Liaoning Key Laboratory of Semiconductor Light Emitting and Photocatalytic Materials.

References

[1] C.H. Tung, L.Z. Wu, L.P. Zhang, B. Chen, Supramolecular systems as microreactors: control of product selectivity in organic phototransformation, Acc. Chem. Res. 36 (2003) 39-47.

[2] G.J. Cramer, D.G. Truhlar. A universal approach to solvation modeling, Acc. Chem. Res. 41 (2008) 760-768.

[3] X. Zhang, L. Chi, S.M. Ji, Y. Wu, P. Song, K.L. Han, H. Guo, T.D. James, J.Z. Zhao, Rational design of de-PeT phenylethynylated-carbazole monoboronic acid fluorescent sensors for the selective detection of α-hydroxyl carboxylic acids and monosaccharides, J. Am. Chem. Soc. 131 (2009) 17452-17463.

[4] G.J. Zhao, K.L. Han, Hydrogen bonding in the electronic excited state, Acc. Chem. Res. 45 (2012) 404-413.

[5] H. Li, H. Yin, X. Liu, Y. Shi, TDDFT assessment of excited state intramolecular proton transfer in a panel of chromophore-2-hydroxypyrene-1-carbaldehyde, J. At. Mol. Sci. 7 (2016) 115-124.

[6] H. Yin, H. Li, G. Xia, C. Ruan, Y. Shi, H. Wang, M. Jin, D. Ding, A novel non-fluorescent excited-state intramolecular proton transfer phenomenon induced by intramolecular hydrogen bonds: an experimental and theoretical investigation, Sci. Rep. 6 (2016) 19774.

[7] Y. Cui, P. Li, J. Wang, P. Song, L. Xia, An investigation of excited-state intramolecular proton transfer mechanism of new chromophore, J. At. Mol. Sci. 6 (2015) 23-33.

[8] J. Zhao, P. Song, F. Ma, A new excited-state intramolecular proton transfer mechanism for C2 symmetry of 10-hydroxybenzoquinoline, Commun. Comput. Chem. 2 (2014) 117-130.

[9] G.Y. Li, G. Zhao, Y.H. Liu, K.L. Han, G.Z. He, TD-DFT study on the sensing mechanism of a fluorescent chemosensor for fluoride: excited-state proton transfer, J. Comput. Chem. 31 (2010) 1759-1765.

[10] M. Eigen, W. Kruse, G. Maass, L. Maeyer, Rate constants of protolytic reactions in aqueous solution, Prog. React. Kinet. 2 (1964) 285-290.

[11] B. Siwick, H. Bakker, On the role of water in intermolecular proton-transfer reactions, J. Am. Chem. Soc. 129 (2007) 13412-13420.

[12] F. Yu, P. Li, B. Wang, K. Han, Reversible near-infrared fluorescent probe introducing tellurium to mimetic glutathione peroxidase for monitoring the redox cycles between peroxynitrite and glutathione in vivo, J. Am. Chem. Soc. 20 (2013) 7674-7680.

[13] F. Yu, P. Li, T. Chu, K. Han, A near-IR reversible fluorescent probe modulated by selenium for monitoring peroxynitrite and imaging in living cells, J. Am. Chem. Soc. 133 (2011) 11030-11033.

[14] H. Ma, J. Huang, Ab initio study of the excited-state proton transfer mechanisms for 3-hydroxy-2-(thiophen-2-yl)chromen-4-one, RSC Adv. 6 (2016) 96147-96153.

[15] K. Enander, L. Choulier, A. Olsson, D. Yushchenko, D. Kanmert, A. Klymchenko, A. Demchenko, Y. Mely, D. Altschuh, A peptide-based, ratiometric biosensor construct for direct fluorescence detection of a protein analyte, Bioconjugated Chem. 19 (2008) 1864-1870.

[16] V. Shvadchak, L. Falomir-Lockhart, D. Yushchenko, T. Jovin. Specificity and kinetics of α-synuclein binding to model membranes determined with fluorescent excited state intramolecular proton transfer (ESIPT) probe, J. Biol. Chem. 286 (2011) 13023-13032.

[17] L. Cong, H. Yin, Y. Shi, M. Jin, D. Ding, Different mechanisms of ultrafast excited state deactivation of coumarin 500 in dioxane and methanol solvents: experimental and theoretical stydy, RSC Adv. 5 (2015) 1205-1212.

[18] K. Tang, M. Chang, T. Lin, H. Pan, T. Fang, K. Chen, W. Hung, Y. Hsu, P. Chou, Fine tuning the energetics of excited-state intramolecular proton transfer (ESIPT): white light generation in a single ESIPT system, J. Am. Chem. Soc. 133 (2011) 17738-17745.

[19] J. Wang, Y. Li, E. Duah, S. Paruchrui, D. Zhou, Y. Pang, A selective NIR-emitting zinc sensor by using Schiff base binding to turn-on excited-state intramolecular proton transfer, J. Mater. Chem. B 2 (2014) 2008-2012.

[20] Z. Zhang, Y. Chen, W. Hung, W. Tang, Y. Hsu, C. Chen, F. Meng, P. Chou, Control of the reversibility of excited-state intramolecular proton transfer (ESIPT) reaction: host-polarity tuning white organic light emitting diode on a new thiazolo[5,4-d]thiazole ESIPT system, Chem. Mater. 28 (2016) 8815-8824.

[21] A. Demchenko, K. Tang, P. Chou, Excited-state proton coupled charge transfer modulated by molecular structure and media polarization, Chem. Soc. Rev. 42 (2013) 1379-1408.

[22] J. Zhao, J. Chen, Y. Cui, J. Wang, L. Xia, Y. Dai, P. Song, F. Ma, A questionable excited-state double-proton transfer mechanism

for 3-hydroxyisoquinoline, Phys. Chem. Chem. Phys. 17 (2015) 1142-1150.

[23] Y. Wang, H. Yin, Y. Shi, M. Jin, D. Ding, Ground-state and excited-state multiple proton transfer via a hydrogen-bonded water wire for 3-hydroxypyridine, New J. Chem. 38 (2014) 4458-4464.

[24] J. Zhao, J. Chen, J. Liu, M. Hoffmann, Competitive excited-state single or double proton transfer mechanisms for bis-2,5-(2-benzoxazolyl)-hydroquinone and its derivatives, Phys. Chem. Chem. Phys. 17 (2015) 11990-11999.

[25] Y. Liu, S. Lan, C. Zhu, S. Lin, Intersystem crossing pathway in quinoline-pyrazole isomerism: a time-dependent density functional theory study on excited-state intramolecular proton transfer, J. Phys. Chem. A 119 (2015) 6269-6274.

[26] L. Yuan, W. Lin, K. Zheng, L. He, W. Huang, Far-red to near infrared analyte-responsive fluorescent probe based on organic fluorophore platforms for fluorescence imaging, Chem. Soc. Rev. 42 (2013) 622-661.

[27] Q. Fei, X. Gu, Y. Liu, B. Shi, H. Liu, G. Xu, C. Li, P. Shi, C. Zhao, Near-infrared fluorescent dyes with large stokes shifts: light generation in BODIPYs undergoing excited state intramolecular proton transfer, Org. Biomol. Chem. 15 (2017) 4072-4076.

[28] M. J. Frisch, G. W. Trucks, H. B. Schlegel, G. E. Scuseria, M. A. Robb, J. R. Cheeseman, G. Scalmani, V. Barone, B. Mennucci, G. A. Petersson, H. Nakatsuji, M. Caricato, X. Li, H. P. Hratchian, A. F. Izmaylov, J. Bloino, G. Zheng, J. L. Sonnenberg, M. Hada, M. Ehara, K. Toyota, R. Fukuda, J. Hasegawa, M. Ishida, T. Nakajima, Y. Honda, O. Kitao, H. Nakai, T. Vreven, J. A. Montgomery Jr, J. E. Peralta, F. Ogliaro, M. Bearpark, J. J. Heyd, E. Brothers, K. N. Kudin, V. N. Staroverov, T. Keith, R. Kobayashi, J. Normand, K. Raghavachari, A. Rendell, J. C. Burant, S. S. Iyengar, J. Tomasi, M. Cossi, N. Rega, J. M. Millam, M. Klene, J. E. Knox, J. B. Cross, V. Bakken, C. Adamo, J. Jaramillo, R. Gomperts, R. E. Stratmann, O. Yazyev, A. J. Austin, R. Cammi, C. Pomelli, J. W. Ochterski, R. L. Martin, K. Morokuma, V. G. Zakrzewski, G. A. Voth, P. Salvador, J. J. Dannenberg, S. Dapprich, A. D. Daniels, O. Farkas, J. B. Foresman, J. V. Ortiz, J. Cioslowski and D. J. Fox, Gaussian 09, revision C.01; Gaussian, Inc., Wallingford, CT, 2009.

[29] C. Lee, W. Yang, R. Parr, Development of the colle-salvetti correlation-energy formula into a functional of the electron density, Phys. Rev. B 37 (1988) 785-789.

[30] W. Kolth, A. Becke, R. Parr, Density functional theory of electronic structure, J. Phys. Chem. 100 (1996) 12974-12980.

[31] F. Furche, R. Ahlrichs, Adiabatic time-dependent density functional methods for excited state properties, J. Chem. Phys. 117 (2002) 7433.

[32] B. Mennucci, E. Cances, J. Tomasi, Evaluation of solvent effects in isotropic and anisotropic dielectrics and in ionic solutions with a unified integral equation method: theoretical bases, computational implementation, and numerical applications, J. Phys. Chem. B 101 (1997) 10506-10517.

[33] E. Cances, B. Mennucci, J. Tomasi, A new integral equation formalism for the polarizable continuum model: theoretical background and applications to isotropic and anisotropic dielectrics, J. Chen. Phys. 107 (1997) 3032.

[34] R. Cammi, J. Tomasi, Remarks on the use of the apparent surface charges (ASC) methods in solvation problems: iterative versus matrix-inversion procedures and the renormalization of the apparent charges, J. Comput. Chem. 16 (1995) 1449-1458.

[35] P. Hobza, Z. Havlas, Blue-shifting hydrogen bonds, Chem. Rev. 100 (2000) 4253-4264.

[36] D. Kosov, P. Popelier, Atomic partitioning of molecular electrostatic potentials, J. Phys. Chem. A 104 (2000) 7339-7345.

[37] J. Zhao, Y. Zheng, Elaboration and controlling excited state double proton transfer mechanism of 2,5-bis(benzoxazol-2-yl)thiophene-3,4-diol, Sci. Rep. 7 (2017) 44897.

[38] J. Zhao, X. Liu, Y. Zheng, Deciphering the excited state behavior for 2-(4'-N,N-Dimethylamonophenyl)imidazo[4,5-b]pyridine, J. Lumin. 188 (2017) 1-6.

[39] G. Zhao, B. Northrop, K. Han, P. Stang, The effect of intermolecular hydrogen bonding on the fluorescence of a bimetallic platinum complex, J. Phys. Chem. A 114 (2010) 9007-9013.

[40] J. Zhao, X. Liu, Y. Zheng, Controlling excited state single versus double proton transfer for 2,2'-bipyridyl-3,3'-diol: solvent effect, J. Phys. Chem. A 121 (2017) 4002-4008.

[41] G. Zhao, J. Liu, L. Zhou, K. Han, Site-selective photoinduced electron transfer from alcoholic solvents to the chromophore facilitated by hydrogen bonding: a new fluorescence quenching mechanism, J. Phys. Chem. B 111 (2007) 8940-8945.

[42] Y. Wang, H. Li, Y. Shi, Evidence for hydrogen-bonded ammonia wire influencing the ESMPT process of the 7-hydroxy-4-methylcoumarin·$(NH_3)_3$ cluster, New J. Chem. 39 (2015) 7026-7032.

[43] C. Miao, Y. Shi, Reconsideration on hydrogen bond strengthening or cleavage of photoexcited coumarin 102 in aqueous solvent: A DFT/TDDFT study, J. Comput. Chem. 32 (2011) 3058-3061.

[44] P. Song, J. Zhao, A possible attributions of excited-state process for PIP and PIP-c system in methanol solvent, Commun. Comput. Chem. 5 (2017) 1-9.

[45] J. Huang, J. Wu, H. Dong, P. Song, J. Zhao, Straightforward stepwise excited state dual proton transfer mechanism for 9-10-HBQ system, Commun. Comput. Chem. 5 (2017) 27-36.

[46] J. Zhao, H. Yao, J. Liu, M. Hoffmann, New excited-state proton transfer mechanisms for 1,8-dihydroxydibenzo[a,h]phenazine, J. Phys. Chem. A 119 (2015) 681-688.

[47] J. Zhao, P. Li, The investigation of ESPT for 2,8-diphenyl-3,7-dihydroxy-4H,6H-pyrano[3,2-g]-chromene-4,6-dione: single or double? RSC Adv. 5 (2015) 73619-73625.

[48] J. Zhao, P. Song, F. Ma, A DFT/TDDFT investigation of excited-state intramolecular proton transfer mechanism of new chromophore, Commun. Comput. Chem. 2 (2015) 146-157.

[49] J. Zhao, P. Li, The effect of acetonitrile solvent on excited-state dynamics for N,N-dimethylanilino-1,3-diketone, Commun. Comput. Chem. 3 (2015) 66-74.

[50] Y. Liu, S. Wang, C. Zhu, S. Lin, A TDDFT study on the excited-state double proton transfer reaction of 8-hydroxyquinoline along a hydrogen-bonded bridge, New J. Chem. 41 (2017) 8437-8442.

[51] Y. Peng, Y. Ye, X. Xiu, S. Sun, Mechanism of excited-state intramolecular proton transfer for 1,2-dihydroxyanthraquinone: effect of water on the ESIPT, J. Phys. Chem. A 121 (2017) 5625-5634.

[52] M. Zhang, Q. Zhou, M. Zhang, Y. Dai, P. Song, Y. Jiang,

Theoretical investigation of the ESIPT mechanism for the 1-hydroxy-9H-fluoren-9-one and 1-Hydroxy-11H-benzo[b]fluoren-11-one chromophores, J. Clust. Sci. 28 (2017) 1191-1200.

[53] J. Zhao, H. Dong, Y. Zheng, Theoretical insights into the excited state double proton transfer mechanism of deep red pigment alkannin, J. Phys. Chem. A 122 (2018) 1200-1208.

[54] D. Yang, J. Zhao, G. Yang, N. Song, R. Zheng, Y. Wang, Elaborating the excited-state proton transfer behaviors for novel 3H-MC and P2H-CH, Org. Chem. Front. 4 (2017) 1935-1942.

[55] Y. Liu, S. Wang, C. Wang, C. Zhu, K. Han, S. Lin, Orientation hydrogen-bonding effect on vibronic spectra of isoquinoline in water solvent: Franck-Condon simulation and interpretation, J. Chem. Phys. 145 (2016) 164314.

[56] Y. Liu, M. Mehata, J. Liu, Excited-state proton transfer via hydrogen-bonded acetic acid (AcOH) wire for 6-hydroxyquinoline, J. Phys. Chem. A 115 (2011) 19-24.

[57] J. Zhao, H. Dong, Y. Zheng, Elaborating the excited state multiple proton transfer mechanism for 9H-pyrido[3,4-b]indole, J. Lumin. 195 (2018) 228-233.

[58] D. Yang, J. Zhao, M. Jia, X. Song, A theoretical study about the excited state intermolecular proton transfer mechanisms for 2-phenylimidazo[4,5-b]pyridine in methanol solvent, RSC Adv. **7** (2017) 34034-34040.

[59] J. Zhao, J. Chen, P. Song, J. Liu, F. Ma, The charge transfer phenomenon in benzene-pyrene-sulfoxide/methanol system: role of the intermolecular hydrogen bond in excited states, J. Clust. Sci. 26 (2015) 1463-1472.

[60] J. Luo, Y. Liu, S. Yang, A. Flourat, F. Allais, K. Han, Ultrafast barrierless photoisomerization and strong ultraviolent absorption of photoproducts in plant sunscreens, J. Phys. Chem. Lett. 8 (2017) 1025-1030.

[61] Y. Saga, Y. Shibata, H. Tamiaki, Spectral properties of single light-harvesting complexes in bacterial photosynthesis, J. Photochem. Photobiol. C. Photochem. Rev. 11 (2010) 15-24.

[62] L. Serrano-Andres, M. Merchan, Are the five natural DNA/RNA base monomers a good choice from natural selection? A photochemical perspective, J. Photochem. Photobiol. C. Photochem. Rev. 10 (2009) 21-32.